Available online at www.sciencedirect.com
ScienceDirect
Journal of Power Sources 176 (2008) 70–75
JOURNAL OF POWER SOURCES
www.elsevier.com/locate/jpowsour

Short communication

Citric acid functionalized carbon materials for fuel cell applications

Chee Kok Poh [a,b], San Hua Lim [a,b], Hui Pan [b], Jianyi Lin [a,b,*], Jim Yang Lee [c]

[a] *Institute of Chemical and Engineering Sciences, 1 Pesek Road, Jurong Island, Singapore 627833, Singapore*
[b] *Department of Physics, National University of Singapore, 2 Science Drive 3, Singapore 117542, Singapore*
[c] *Department of Chemical and Biomolecular Engineering, National University of Singapore, 10 Kent Ridge Crescent, Singapore 119260, Singapore*

Received 20 August 2007; received in revised form 18 September 2007; accepted 11 October 2007
Available online 23 October 2007

Abstract

Carbon materials can be easily functionalized using citric acid (CA) treatment. The CA modification of carbon materials is both simple and effective. It requires no prolonged heating, filtration and washing, and produces more functional groups such as carboxyl and hydroxide on CA-modified carbon nanotubes and XC72 carbon blacks than on HNO_3–H_2SO_4 oxidized carbon nanotubes and as-purchased XC72. Platinum nanoparticles are deposited on these functionalized carbon materials by means of a microwave-assisted polyol process. The investigations using TEM, XRD, FTIR and TGA indicate that CA modification creates more functional groups and thus deposits more Pt nanoparticles with smaller average particle size on the surface of carbon materials. Electrochemical studies of the Pt/C samples for methanol oxidation reveal higher activity for Pt on CA-modified carbon materials. It is therefore considered that this method can find important applications in reducing the cost and improving performance of proton-exchange membrane fuel cells.

Keywords: Platinum nanoparticle electrocatalyst; Functionalization of carbon materials; Methanol electro-oxidation; Citric acid; Proton-exchange membrane fuel cell

1. Introduction

Following the discovery of carbon nanotubes [1], their unique mechanical, electrical and structural properties have attracted much attention. Investigations have been conducted to find applications for carbon nanotubes in hydrogen storage [2,3], electrochemical energy storage [4], electronic devices [5,6], and heterogeneous catalysis [7–9]. A number of studies have shown that carbon nanotubes can provide a better support for Pt catalysts in proton-exchange membrane fuel cells (PEMFCS) compared with traditional carbon black [10–13]. Matsumoto et al. [14] reported that by using multi-walled carbon nanotubes (MWCNTs) as a catalyst support in a hydrogen/oxygen fuel cell, 12 wt.% Pt-deposited carbon nanotubes electrode gave 10% higher voltages than a 29 wt.% Pt-deposited carbon black electrode and reduced Pt usage by 60% [14]. Li et al. [15] demonstrated that Pt catalysts deposited on MWCNTs showed higher activity in a direct methanol fuel cell in a high current density region (i.e. at 0.4 V) as compared with that on commercial XC72 carbon black, with 37% higher current density under the same test conditions [15].

To enhance the attachment of nano-sized Pt particles on a carbon support, surface functionalization of the carbon support is often helpful. The oxidation of carbon nanotubes with HNO_3, $KMnO_4$, H_2O_2 or ozone gas (O_3) has been found to introduce functional groups such as hydroxyl (–OH), carboxyl (–COOH), carbonyl (–CO) and sulfate (–OSO_3H) groups [16–22] on the surfaces of carbon nanotubes and thereby provide nucleation sites for the deposition of highly dispersed metal particles. These surface oxidation methods, however, often require extensive (usually 4–48 h [23–25]) heating, filtration and washing to remove the oxidant. In a previous study [26], we used citric acid (CA) to create functional groups on carbon nanotubes for the subsequent uniform dispersion of gold nanoparticles. The surface modification of MWCNTs by CA was done simply by heating a CA/MWCNTs mixture at 300 °C for 0.5 h, with

* Corresponding author at: Institute of Chemical and Engineering Sciences, 1 Pesek Road, Jurong Island, Singapore 627833, Singapore. Tel.: +65 6796 3807; fax: +65 6316 6182.
E-mail addresses: poh_chee_kok@ices.a-star.edu.sg (C.K. Poh), lim_san_hua@ices.a-star.edu.sg (S.H. Lim), phyph@nus.edu.sg (H. Pan), Lin_Jianyi@ices.a-star.edu.sg (J. Lin), cheleejy@nus.edu.sg (J.Y. Lee).

0378-7753/$ – see front matter © 2007 Elsevier B.V. All rights reserved.
doi:10.1016/j.jpowsour.2007.10.049

no post-washing and filtrating, since the thermal decomposition temperature of CA is 175 °C.

In this study, the above CA-treatment is employed to functionalize MWCNTs and commercial carbon blacks (XC72). When CA-functionalized MWCNTs and XC72 are used as supports for Pt deposition, higher Pt loading, smaller particle-size and higher electrochemical activity are measured by thermogravimetric analysis (TGA), transmission electron microscope (TEM) and cyclic voltammetry (CV), in comparison with acid-refluxed MWCNTs and XC72 under identical experimental conditions. These results indicate that CA modification is a promising technique of electrocatalyst preparation for fuel cell applications.

2. Experimental methods

2.1. CA Treatment of MWCNTs and XC72

In a typical experiment, 100 mg of MWCNTs (Shenzhen Nanotech Co. Ltd., with diameters between 20 and 40 nm), 100 mg of citric acid monohydrate (Fluka 99.5%) and 10 mL of distilled water were mixed with the assistance of ultrasonic vibration (Elma, 100W and 35 kHz) for 15 min, and then left to dry to form a paste. After heating at 300 °C for 30 min, the CA-treated MWCNTs were ready for Pt deposition. The same procedure was repeated for XC72 carbon blacks (Cabot Corp.).

2.2. Deposition of platinum nanoparticles on MWCNTs and XC72

Forty milligrams of the above functionalized MWCNTs were dispersed in 50 mL of ethylene glycol (Sigma–Aldrich 99+%) by ultrasonic vibration and mixed with 1.0 mL of 0.04 M $H_2PtCl_6{\cdot}6H_2O$ (Fluka) aqueous solution in a Teflon vessel. 0.5 mL of 0.8 M NaOH was added drop-wise into the mixture and stirred vigorously. The mole ratio of NaOH:Pt was >8 to induce the formation of small and uniform Pt particles [27]. The Teflon vessel with the mixture was placed inside a Milestone MicroSYNTH programmable microwave system (1000 W, 2.45 GHz), heated to 160 °C within 2 min, and maintained at the same temperature for another 2 min for the reduction of the platinum precursor. The resulting suspension of Pt-deposited carbon nanotubes was centrifuged, washed with acetone to remove the organic solvent, and dried at 80 °C overnight in a vacuum oven.

For comparison, the deposition of Pt nanoparticles was also conducted on acid-refluxed MWCNTs, CA-modified XC72 and as-purchased carbon blacks (XC72, Cabot Corp.) under the same conditions described above. The acid-refluxed MWCNTs were prepared by refluxing the MWCNTs with a concentrated H_2SO_4–HNO_3 acid mixture (3:1 v/v) for 5 h, followed by filtration, washing of the resulting mixture, and drying in a vacuum oven.

2.3. Catalyst characterization

The particle-size distribution of the platinum was examined by means of a transmission electron microscope (JEOL JEM2010F) that operated at 200 kV. A total of 400 Pt nanoparticles were counted in each sample to ensure a statistically representative analysis of the particle distribution.

The platinum loading of the catalyst was determined by thermogravimetric analysis (Setaram TGA equipment). Several milligrams of the Pt–carbon samples were heated to 800 °C in a flow of purified oxygen.

Infrared transmission spectra were measured with a Perkin-Elmer 2000 Fourier-transform infrared spectrometer (FTIR) in the range of 400–4000 cm^{-1}.

X-ray diffraction (XRD) measurements were carried out with a Bruker D8 advance x-ray diffractometer, which was scanned from $2\theta = 10°$ to 90°. The average crystallite size of the Pt particles was estimated from the diffraction peak of Pt(1 1 1) using the Debye–Scherrer equation [28], i.e.,

$$d = 0.9\lambda_{k\alpha1}/B\cos\theta_{max} \quad (1)$$

in which d is the average size of the Pt particle, $\lambda_{k\alpha1}$ the X-ray wavelength (Cu Kα $\lambda_{k\alpha1}$ = 1.5418 Å), θ_{max} the maximum angle of the (1 1 1) peak, and B is the full-width at half-maximum in radians.

2.4. Electrochemical measurements

Cyclic voltammetry (CV) measurements were performed with Solartron SI1280B equipment, a combined electrochemical interface and frequency response analyzer, at room temperature at a scan rate of 50 mV s^{-1}. The working electrode was fabricated by casting a Nafion-impregnated catalyst ink onto a glassy carbon electrode (3 mm diameter). Typically, 8 mg of the Pt–C catalyst dispersed in 0.5 mL of ethanol aqueous solution (1:1 v/v) was sonicated for 15 min and 60 μL of a 5 wt.% Nafion solution was added as polymer binder [29]. 3.4 μL of this catalyst ink was dropped onto the glassy carbon electrode. The electrode was placed and in a vacuum oven until the catalyst was totally dry. For CV measurements the catalyst cast working electrode was immersed in 0.5 M H_2SO_4 with or without 1 M CH_3OH, which was purged with high purity nitrogen gas for electrochemical measurement. A Pt foil and a saturated calomel electrode (SCE) were used as counter electrode and reference electrode, respectively.

3. Results and discussion

3.1. TEM analysis

Fig. 1 shows TEM images of Pt nanoparticles supported on different carbon supports. The histograms in Fig. 2 give the mean particle size of Pt, namely, approximately 2.9, 3.1, 2.3 and 6.1 nm for Pt/MWCNTs (CA modified) (Fig. 2a), Pt/MWCNTs (acid refluxed) (Fig. 2b) and Pt/XC72 (CA modified) (Fig. 2c) and Pt/XC72 (Fig. 2d), respectively. The density of Pt particle numbers on the carbon supports, estimated from the TEM images, is around 3.3×10^{16} m^{-2} for Pt/MWCNTs (CA modified), 1.3×10^{16} m^{-2} for Pt/MWCNTs (acid refluxed), 5.43×10^{16} m^{-2} for Pt/XC72 (CA modified),

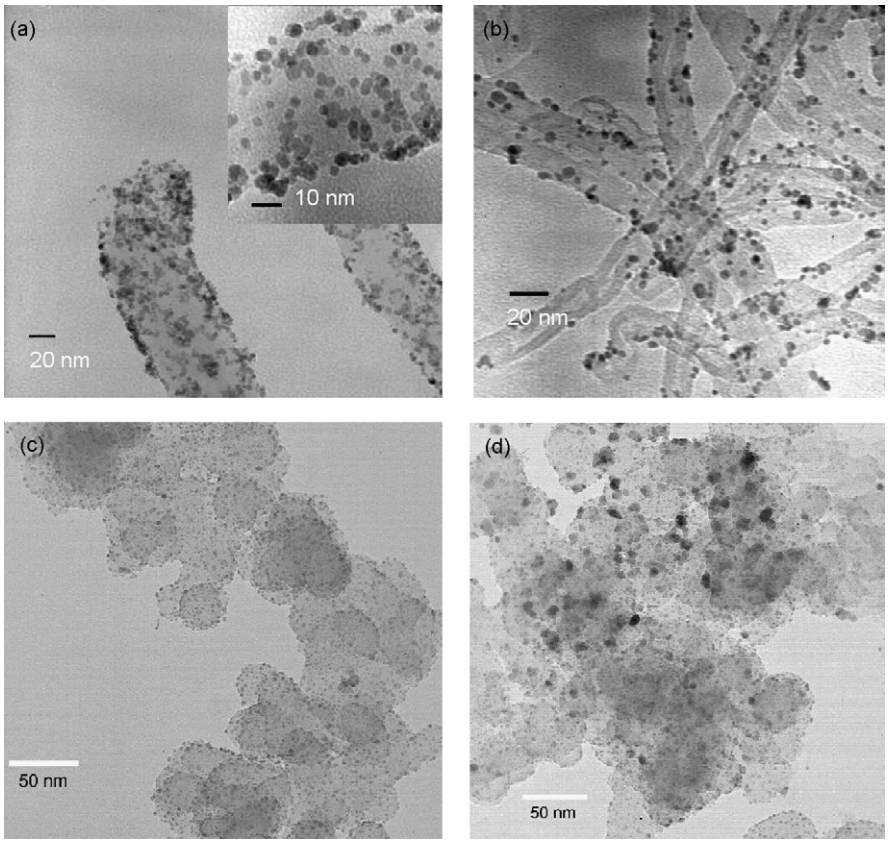

Fig. 1. TEM images of: (a) Pt/MWCNTs (CA modified); (b) Pt/MWCNTs (acid refluxed); (c) Pt/XC72 (CA modified); (d) Pt/XC72.

and 1.94×10^{16} m^{-2} for Pt/XC72, respectively. Under identical preparation procedures, a high Pt particle number per unit area and small particle sizes are significantly important in fuel cell applications since these factors may increase Pt utilization and reduce the limitations of mass transport and ohmic resistance [30,31].

The above results show that Pt dispersion on the carbon support is in the order: XC72(CA modified) > MWCNTs(CA modified) > MWCNTs(acid refluxed) > XC72. The homogeneous dispersion of Pt nanoparticles on the carbon nanotubes is attributed to the presence of functional groups on the surface [22,32]. Similarly the poorer dispersion of Pt nanoparticles on as-purchased XC72 may be due to a relatively lower concentration of functional groups on the surface. Obviously, the CA functionalization of carbon materials is effective in enhancing the surface density of Pt nanoparticles.

3.2. XRD Characterization

The above TEM measurements can be further confirmed by X-ray powder diffraction (XRD). The XRD patterns of the catalysts are given in Fig. 3. The C(2 0 0) peak is much stronger and sharper for Pt/MWCNTs than for Pt/XC72 due to the superior graphitization of MWCNTs. The diffraction peaks at 39.6°, 46.3°, 67.4°, 81.4°, and 85.4° are assigned to Pt(1 1 1), Pt(2 0 0), Pt(2 2 0), Pt(3 1 1), and Pt(2 2 2), respectively. The average size of the Pt particles, as determined by the Sherrer formula, is 2.5 nm for Pt/MWCNTs (CA/MWCNTs modified), 3.9 nm for Pt/MWCNTs (acid refluxed)), 6.4 nm for Pt/XC72, and 2.4 nm for Pt/XC72 (CA modified)), that is, very close to the average particle sizes obtained from the TEM investigations.

3.3. TGA analysis

Fig. 4 displays TGA weight-loss curves that were obtained upon heating Pt:carbon in oxygen. The carbon supports are burned mainly at 650 °C (curve I), 625 °C (curve II), 560 °C (curve III) and 511 °C (curve IV) for MWCNTs (CA modified), MWCNTs (acid refluxed), XC72 and XC72 (CA modified), respectively. The MWCNTs are more difficult to burn than XC72 due to better graphitization. During oxidation, deposited Pt is converted to platinum oxides in the residual ash. The Pt loading is estimated to be 15.4 wt.% on CA-modified MWCNTs as compared with 12.6 wt.% on acid refluxed MWCNTs, 13.0 wt.% on XC72 and 14.6 wt.% on CA-modified XC72. Since the four Pt–C samples were prepared under otherwise identical conditions with the same amount of Pt precursors, the fact that Pt/MWCNTs (CA modified) and Pt/XC72 (CA modified) have a higher loading, but smaller Pt nanoparticles, implies that CA modification allow to anchor more Pt particles and disperses them better on carbon supports. This is significantly important in reducing the Pt loading and improving the Pt catalytic performance.

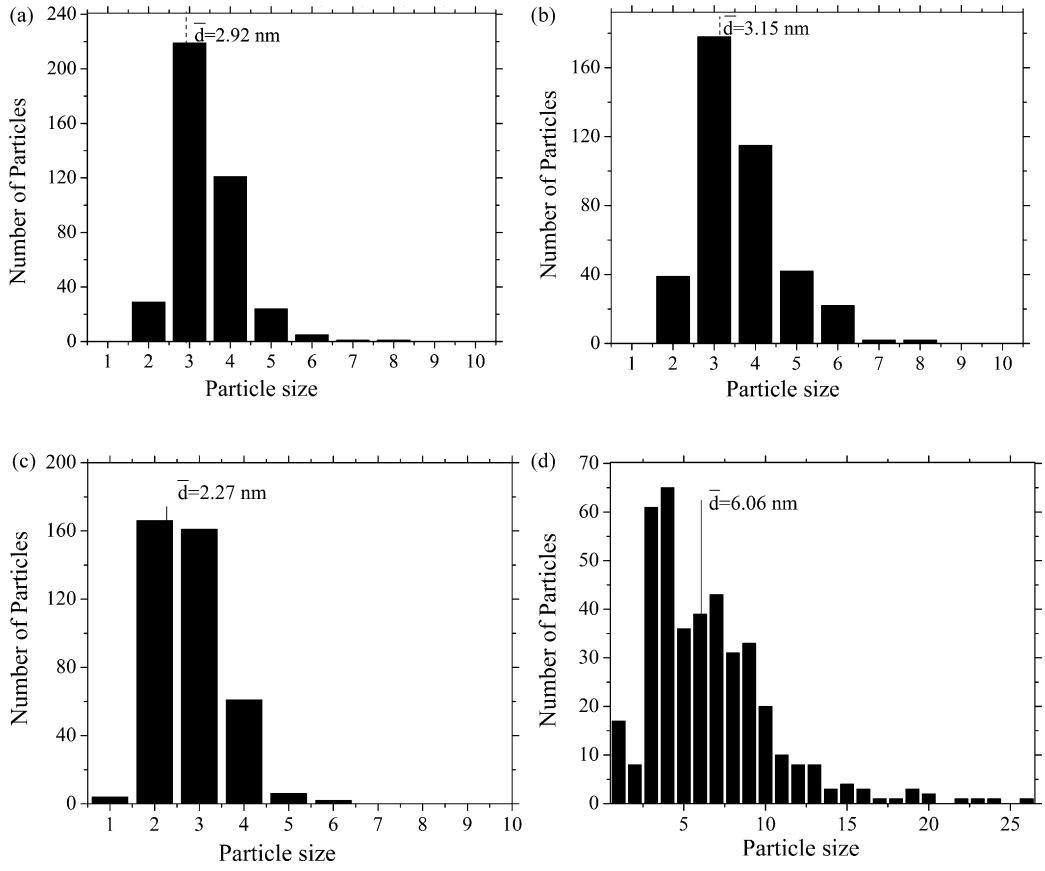

Fig. 2. Size distribution of Pt nanoparticles supported on: (a) CA-modified MWCNTs; (b) acid refluxed MWCNTs; (c) CA-modified XC72; (d) as-purchased XC72.

3.4. FTIR analysis

The FTIR spectra in Fig. 5 clearly show the existence of carbonyl and carboxylic groups at wavenumbers 1300–1700 cm^{-1} and hydroxyl bands at wavenumbers 3300–3500 cm^{-1} on all the carbon materials. The spectrum 2 is for the MWCNTs sample which was subjected to a similar heating treatment with no addition of CA. Compared with this, the CA-treated MWCNTs sample shows strong IR bands at 1630 and 1380 cm^{-1}, which can be assigned to asymmetric and symmetric $HCOO^-$ stretching (see spectrum 4, Fig. 5a). This is in accordance with the fact that CH_2COOH is part of the citric acid molecule. An IR band is not found at 1380 cm^{-1} in spectrum 2 of Fig. 5a, which confirms that the functional groups are largely caused by CA and not by merely heating in water. As shown in Fig. 5b, the intensification and broadening of the IR adsorption bands of XC72 after CA modification clearly demonstrates

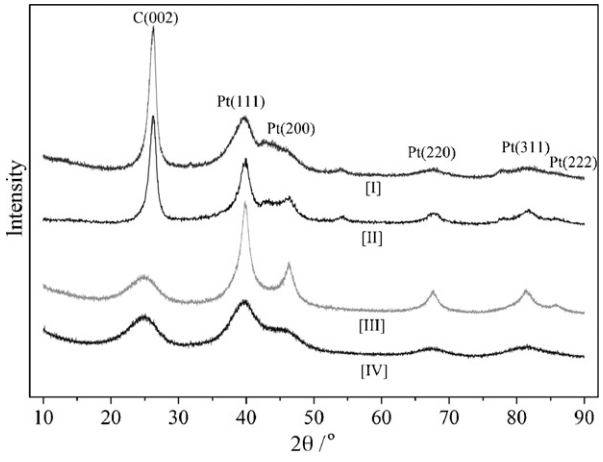

Fig. 3. XRD patterns for Pt catalyst supported on: [I] MWCNTs (CA modified); [II] MWCNTs (acid refluxed); [III] XC72; [IV] XC72 (CA modified).

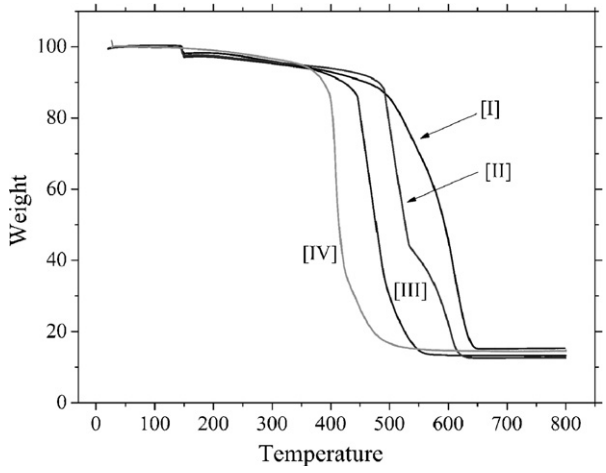

Fig. 4. TG weight loss curves for Pt/MWCNTs (CA modified) (curve I); Pt/MWCNTs (acid refluxed) (curve II); Pt/XC72 (curve III); Pt/XC72 (CA modified) (curve IV).

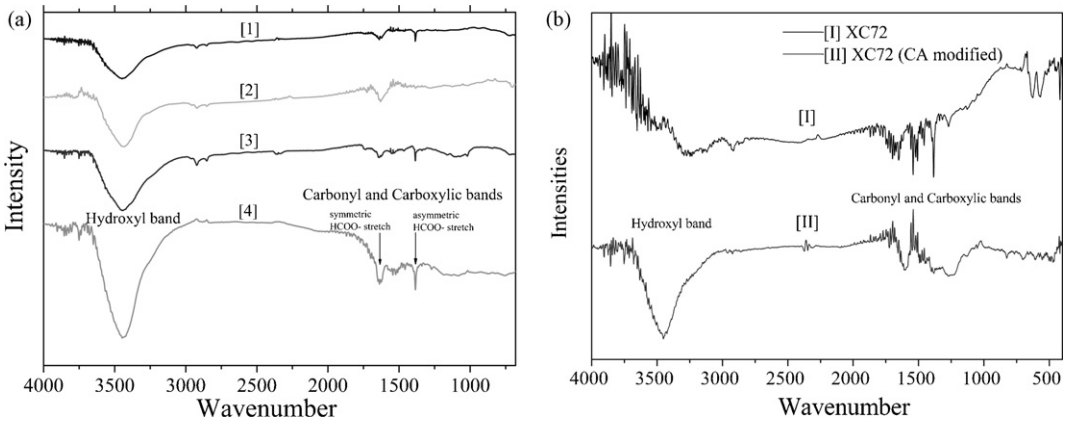

Fig. 5. FTIR spectra of: (a) MWCNTs (as-received), MWCNTs (heated w/o CA), MWCNTs (acid refluxed) and MWCNTs (CA modified), respectively, from top to bottom and (b) XC72 and XC72 (CA modified).

that more functional groups are attached to the CA-modified XC72.

3.5. Evaluation of electrochemical active surface area

Cyclic voltammetry (CV) curves were obtained for the Pt catalysts on four different carbon supports in the potential range of −0.2–1.0 V (vs. a reference saturated calomel electrode). In Fig. 6a, it can be seen that Pt/MWCNTs (both CA modified and acid refluxed) and Pt/XC72 (CA modified) produce much higher current density in the hydrogen adsorption/desorption region (−0.2–0.16 V) than Pt/XC 72. The capacitive current in the CV curves of the Pt/MWCNTs catalyst (both CA modified and acid refluxed) is also higher than commercial carbon black due to the high specific capacitance of carbon nanotubes [33,34].

The electrochemical active surface area of all the four Pt/C catalysts can be estimated from the hydrogen adsorption/desorption peaks of the cyclic voltammograms in Fig. 6. Assuming a hydrogen monolayer adsorption charge of $Q_H^0 = 210\,\mu C\,cm^{-2}$ [35], the electrochemical active surface area (EAS) is given by $S_{ec} = Q_H/Q_H^0$ where Q_H is the average specific charge derived from the hydrogen adsorption/desorption peak area in the CV curve [26]. The EAS is 73.82, 70.71, 43.45 and 76.02 $m^2\,g^{-1}$ for Pt/MWCNTs (CA modified), Pt/MWCNTs (acid refluxed), Pt/XC72 and Pt/XC72 (CA modified), respectively. Compared with the high electrochemical surface area of the functionalized MWCNTs and XC72, the EAS of Pt/XC72 is rather low, due to the large average particle size and poor dispersion of the Pt nanoparticles.

Cyclic voltammograms for methanol oxidation on the catalysts over the potential range of −0.2–1.0 V (vs. SCE) are presented in Fig. 6b, in which two peaks of methanol oxidation can be observed, i.e., E_{p1} (0.65–0.67 V) in the forward scan and E_{p2} (0.44–0.46 V) in the reverse scan. The shape of the CV and the peak potentials are in accordance with other studies [36,37]. The specific current generated by Pt/MWCNTs (CA modified) at E_{p1}, which corresponds to methanol electroxidation, is 0.64 A $(mgPt)^{-1}$. This is about 2.5 times as large as that of Pt/XC72 and 1.5 times of Pt/MWCNTs (acid refluxed). Pt/XC72 (CA modified) (curve IV in Fig. 6b) also shows an oxidation peak which is higher. Pt/MWCNTs (CA modified) and much higher than those of Pt/MWCNTs (acid refluxed) and Pt/XC72.

3.6. Analysis of functional group influence

The high activity of Pt/MWCNTs (CA modified) and Pt/XC72 (CA modified) may be attributed to a higher Pt surface density, better Pt dispersion, and the existence of functional

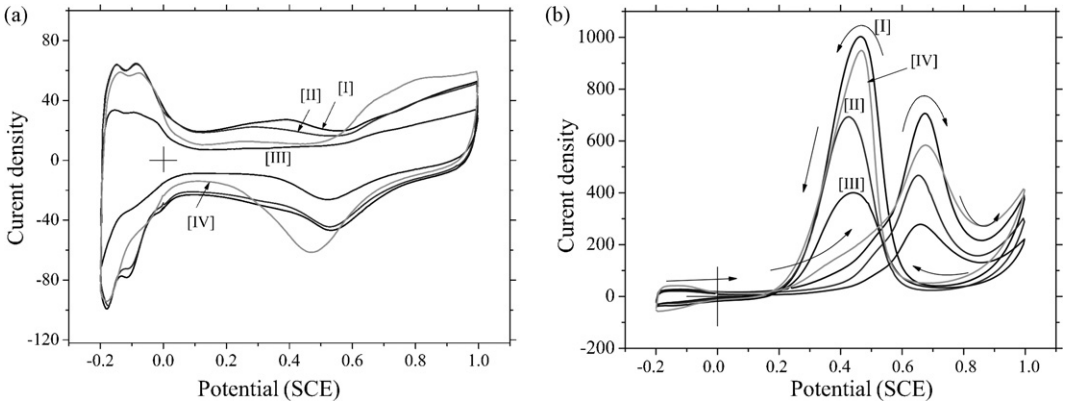

Fig. 6. (a) Cyclic voltammograms for: Pt/MWCNTs (CA modified) (curve I); Pt/MWCNTs (acid refluxed) (curve II); Pt/XC72 (curve III); Pt/XC72 (CA modified) (curve IV). Scan rate = 50 mV s^{-1} at room temperature in 0.5 M H_2SO_4. (b) Cyclic voltammograms of: Pt/MWCNTs (CA modified) (curve I); Pt/MWCNTs (acid refluxed) (curve II); Pt/XC72 (curve III); Pt/XC72 (CA modified) (curve IV). Scan rate = 50 mV s^{-1} at room temperature in 1 M CH_3OH + 0.5 M H_2SO_4.

groups attached to the carbon materials surface. According to the *ab initio* density-functional-theory calculations by Britto et al. [38], electrodes of carbon nanotubes can improve the charge-transfer process due to the unique structure of the carbon nanotubes. The functional groups attached to the walls of the carbon nanotubes have been found to enhance further their conductivity [39]. More importantly, the increase in the number of surface hydroxyl groups by CA treatment might facilitate the removal of the CO intermediate that is adsorbed on Pt surface during the electro-oxidation of methanol on Pt catalysts which may proceed via the following scheme [40]:

$$Pt + CH_3OH \rightarrow Pt\text{–}CO_{ads} + 4H^+ + 4e^- \quad (2)$$

$$Pt + H_2O \rightarrow Pt\text{–}OH_{ads} + H^+ + e^- \quad (3)$$

$$Pt\text{–}CO_{ads} + Pt - OH_{ads} \rightarrow CO_2 + H^+ + e^- \quad (4)$$

On a pure-Pt electrode, the rate of stripping the CO intermediate from Pt sites is low since the adsorption of the OH intermediate on Pt is difficult [41]. The presence of a high concentration of hydroxyl groups on the CA-modified carbon supports can facilitate the removal of CO, and thus the oxidation of methanol, to yield a higher oxidation current compared with carbon supports without CA treatment. As shown in Fig. 6b, the current peaks in the reverse scan, which are related to the oxidation of CO intermediates [42], are higher for Pt/MWCNTs (CA modified) and Pt/XC72 (CA modified).

4. Conclusions

This investigation presents a simple and efficient method for the preparation of highly dispersed Pt nanoparticles on carbon materials. CA-modified MWCNTs and XC72 are shown by FTIR analysis to have more functional groups on their surfaces as compared with acid refluxed MWCNTs and as-purchased XC72. TEM and TGA studies measure higher Pt density and better Pt dispersion on CA-modified MWCNTs and XC72. From CV examination of methanol oxidation in 0.5 M sulfuric acid, Pt nanoparticles supported on CA-modified MWCNTs and XC72 have higher electrochemical activity than Pt supported on acid refluxed MWCNTs and as-purchased XC72. This is a result of the higher density of functional groups produced by the CA method. A high density of functional groups can facilitate the dispersion of Pt catalysts and may enhance the removal of CO intermediates during the electro-oxidation of methanol.

References

[1] S. Ijima, Nature 354 (1991) 56–58.
[2] H. Gao, X.B. Wu, J.T. Li, G.T. Wu, J.Y. Lin, K. Wu, D.S. Xu, Appl. Phys. Lett. 83 (2003) 3389–3391.
[3] G.P. Dai, C. Liu, M. Liu, M.Z. Wang, H.M. Cheng, Nano Lett. 2 (2002) 503–506.
[4] E. Frackowiak, F. Béguin, Carbon 40 (2002) 1775–1787.
[5] S. Fan, M.G. Chapline, N.R. Franklin, T.W. Tombler, A.M. Cassell, H. Dai, Science 283 (1999) 512–514.
[6] S. Frank, P. Poncharal, Z.L. Wang, W.A. de Heer, Science 280 (1998) 1744–1746.
[7] J.M. Planeix, N. Couste, B. Coq, V. Brotons, P.S. Kumbhar, R. Dutartre, P. Geneste, P. Bernier, P.M. Ajayan, J. Am. Chem. Soc. 116 (1994) 7935–7936.
[8] W. Li, C. Liang, W. Zhou, J. Qiu, H. Li, G. Sun, Q. Xin, Carbon 42 (2004) 436–439.
[9] K. Jiang, A. Eitan, L.S. Schadler, P.M. Ajayan, R.W. Siegel, N. Grobert, M. Mayne, M. Reyes-Reyes, H. Terrones, M. Terrones, Nano Lett. 3 (2003) 275–277.
[10] T. Matsumoto, T. Komatsu, H. Nakano, K. Arai, Y. Nagashima, E. Yoo, T. Yamazaki, M. Kijima, H. Shimizu, Y. Takasawa, J. Nakamura, Catal. Today 90 (2004) 277–281.
[11] M. Carmo, V.A. Paganin, J.M. Rosolen, E.R. Gonzalez, J. Power Sources 142 (2005) 169–176.
[12] Z. Liu, X. Lin, J.Y. Lee, W. Zhang, M. Han, L.M. Gan, Langmuir 18 (2002) 4054–4060.
[13] W. Li, C. Liang, J. Qiu, W. Zhou, H. Han, Z. Wei, G. Sun, Q. Xin, Carbon 40 (2002) 787–803.
[14] T. Matsumoto, T. Komatsu, K. Arai, T. Yamazaki, M. Kijima, H. Shimizu, Y. Takasawa, J. Nakamura, Chem. Commun. 7 (2004) 840–841.
[15] W. Li, C. Liang, W. Zhou, J. Qiu, Z. Zhou, G. Sun, Q. Xin, J. Phys. Chem. B 107 (2003) 6292–6299.
[16] J. Liu, A.G. Rinzler, H. Dai, J.H. Hafner, R.K. Bradley, P.J. Boul, A. Lu, T. Iverson, K. Shelimov, C.B. Huffman, F. Rodriguez-Macias, Y.S. Shon, T.R. Lee, D.T. Colbert, R.E. Smalley, Science 280 (1998) 1253–1256.
[17] T. Kyotani, S. Nakazaki, W.H. Xu, A. Tomita, Carbon 39 (2001) 782–785.
[18] D.B. Mawhinney, V. Naumenko, A. Kuznetsova Jr., J.T. Yates, J. Liu, R.E. Smalley, J. Am. Chem. Soc. 122 (2000) 2383–2384.
[19] K. Hernadi, A. Siska, L. Thien-Nga, L. Forro, I. Kiricsi, Solid State Ionics 141/142 (2001) 203–209.
[20] Z. Chen, R.H. Hauge, R.E. Smalley, J. Nanosci. Nanotechnol. 6 (2006) 1935–1938.
[21] R. Yu, L. Chen, Q. Liu, J. Lin, K.L. Tan, S.C. Ng, H.S.O. Chan, G.Q. Xu, A.T.S. Hor, Chem. Mater. 10 (1998) 718–722.
[22] D.J. Guo, H.L. Li, Electroanal 17 (2005) 869–872.
[23] Y. Xing, J. Phys. Chem. B 108 (2004) 19255–19259.
[24] J. Zhang, H. Zou, Q. Qing, Y. Yang, Q. Li, Z. Liu, X. Guo, Z. Du, J. Phys. Chem. B 107 (2003) 3712–3718.
[25] V. Lordi, N. Yao, J. Wei, Chem. Mater. 13 (2001) 733–737.
[26] S.H. Lim, J. Wei, J. Lin, Chem. Phys. Lett. 400 (2004) 578–582.
[27] W. Yu, W. Tu, H. Liu, Langmuir 15 (1999) 6–9.
[28] E. Antolini, F. Cardellini, J. Alloys Comp. 315 (2001) 118–122.
[29] G. Li, P.G. Pickup, J. Electrochem. Soc. 150 (2003) C745–C752.
[30] S. Srinivasan, D.J. Manko, H. Koch, M.A. Enayetullah, A.J. Appleby, J. Power Sources 29 (1990) 367–387.
[31] Z. Shao, B. Yi, M. Han, J. Power Sources 79 (1999) 82–85.
[32] J.V. Zoval, J. Lee, S. Gorer, R.M. Penner, J. Phys. Chem. B 102 (1998) 1166–1175.
[33] J.H. Chen, W.Z. Li, D.Z. Wang, S.X. Yang, J.G. Wen, Z.F. Ren, Carbon 40 (2002) 1193–1197.
[34] Y. Xing, L. Li, C.C. Chusuei, R.V. Hull, Langmuir 21 (2005) 4185–4190.
[35] B. Le Gratiet, H. Remita, G. Picq, M.O. Delcourt, J. Catal. 164 (1996) 36–43.
[36] K.E. Swider, D.R. Rolison, J. Electrochem. Soc. 143 (1996) 813–819.
[37] H. Tang, J. Chen, S. Yao, L. Nie, Y. Kuang, Z. Huang, D. Wang, Z. Ren, Mater. Chem. Phys. 92 (2005) 548–553.
[38] P.J. Britto, K.S.V. Santhanam, A. Rubio, J.A. Alonso, P.M. Ajayan, Adv. Mater. 11 (1999) 154–157.
[39] H. Pan, Y.P. Feng, J. Lin, Phys. Rev. B 70 (2004), 245425-1–245425-5.
[40] A. Kabbabi, R. Faure, R. Durand, B. Beden, F. Hahn, J.M. Leger, C. Lamy, J. Electroanal. Chem. 444 (1998) 41–53.
[41] A. Perez, M.J. Vilkas, C.R. Cabrera, Y. Ishikawa, J. Phys. Chem. B 109 (2005) 23571–23578.
[42] J. Lee, C. Eickes, M. Eiswirth, G. Ertl, Electrochim. Acta 47 (2002) 2297–2301.